HHS Public Access

Author manuscript

Traffic. Author manuscript; available in PMC 2016 December 01.

Published in final edited form as:

Traffic. 2015 December ; 16(12): 1239–1253. doi:10.1111/tra.12332.

Identification of a VxP targeting signal in the flagellar Na^+/K^+-ATPase

Joseph G. Laird[1], **Yuan Pan**[1,*], **Modestos Modestou**[1], **David M. Yamaguchi**[1], **Hongman Song**[2,#], **Maxim Sokolov**[2], and **Sheila A. Baker**[1]

[1]Department of Biochemistry, Carver College of Medicine, University of Iowa, Iowa City, Iowa 52242, USA

[2]Department of Ophthalmology, West Virginia University School of Medicine and West Virginia University Eye Institute, Morgantown, West Virginia 26506, USA

Abstract

Corresponding Author: Sheila A Baker, Biochemistry, 4-712 BSB, 51 Newton Road, University of Iowa, Iowa City, IA 52242, Phone 319-353-4119, Fax 319-335-9570, sheila-baker@uiowa.edu.

*Current address: Department of Neurology, Washington University School of Medicine, St. Louis, MO 63110, USA

#Current address: Section for Translational Research in Retina & Macular Degeneration, National Institute on Deafness and Other Communication Disorders, NIH, Bethesda, MD 20892, USA

The authors have no conflict of interest to declare.

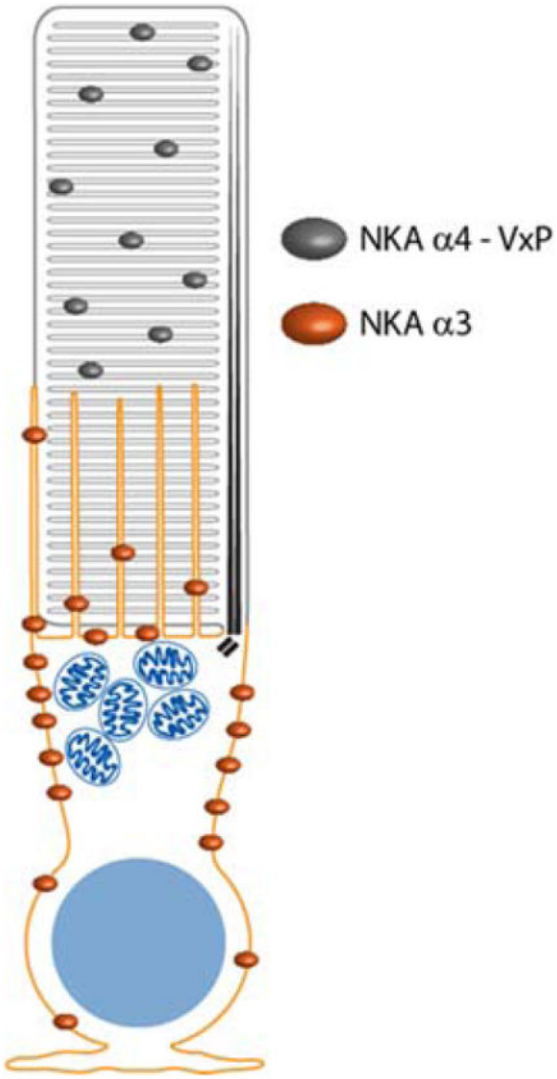

Na^+/K^+-ATPase (NKA) participates in setting electrochemical gradients, cardiotonic steroid signaling, and cellular adhesion. Distinct isoforms of NKA are found in different tissues and subcellular localization patterns. For example, NKA α1 is widely expressed, NKA α3 is enriched in neurons, and NKA α4 is a testes specific isoform found in sperm flagella. In some tissues, ankyrin, a key component of the membrane cytoskeleton, can regulate the trafficking of NKA. In the retina, NKA and ankyrin-B are expressed in multiple cell types and immunostaining for each is striking in the synaptic layers. Labeling for NKA is also prominent along the inner segment plasma membrane of photoreceptors. NKA co-immunoprecipitates with ankyrin-B, but on a subcellular level co-localization of these two proteins varies dependent on the cell type. We used transgenic *X. laevis* tadpoles to evaluate the subcellular trafficking of NKA in photoreceptors. GFP-NKA α3 and α1 localized to the inner segment plasma membrane, but α4 localized to outer segments. We identified a VxP motif responsible for the outer segment targeting by using a series of chimeric and mutant NKA constructs. This motif is similar to previously identified ciliary targeting motifs. Given the structural similarities between outer segments and flagella, our findings shed light on the subcellular targeting of this testes specific NKA isoform.

Keywords

ATPase; ATP1a3; ATP1a4; ankyrin; photoreceptors; Muller glia; synapse; retina; cilia; sperm; flagella; trafficking

INTRODUCTION

Na^+/K^+-ATPase (NKA) is the ubiquitously expressed sodium pump responsible for maintaining electrochemical gradients across cellular membranes. It is one of the major consumers of ATP in the body; ATP hydrolysis is coupled to the active transport of three Na^+ ions out, and two K^+ ions into the cell. NKA also serves as a receptor for cardiotonic steroids and neuronal agrin, thus, is involved in a number of cellular signaling pathways (1–3). Yet another distinct role for NKA is in cellular adhesion (4). For instance, in the retina, NKA is the receptor for the secreted factor, retinoschisin (5, 6). Retinoschisin is a protein disrupted in X-linked juvenile retinoschisis, a progressive degenerative disease characterized by splitting of the layers of the retina and consequently decreased neurotransmission from photoreceptors to bipolar cells (7). Given these diverse roles, it is not surprising that there is heterogeneity in the composition and subcellular localization of NKA throughout the body.

NKA is a heteromeric multispanning membrane protein composed of a catalytic α subunit and a heavily glycosylated β subunit. NKA β is necessary for proper assembly and trafficking of the enzyme. In some tissues, a third regulatory subunit (γ) belonging to the FXYD family of proteins modulates the activity of the enzyme. There are four, three, and seven genes for the α, & beta;, and γ subunits respectively. The α subunits have overlapping but distinct expression patterns that is likely important for supporting the subtly different functions of the NKA subunits reflected by the diseases that manifest as a result of their mutation. NKA α1 (encoded by *ATP1A1*) is the most widely expressed catalytic subunit. Not surprisingly, the *ATP1A1* knockout mouse is embryonic lethal (8). But more discrete mutations in this gene can lead to aldosterone-producing adenomas and hypertension (9–11). NKA α2 is enriched in cardiac muscle, skeletal muscle, and the brain; mutations in *ATP1A2* are linked to migraine (12). NKA α3 is enriched in nervous tissue and mutations in *ATP1A3* cause the movement disorders, rapid-onset dystonia parkinsonism or alternating hemiplegia of childhood, type 2 (13, 14). NKA α4 is uniquely expressed in mammalian testes and consequently is required for fertility (15–18). Multiple transcriptional and signaling mechanisms converge to control the differential tissue expression of NKA (19–26).

NKA can also be controlled by differential subcellular localization in a cell-type specific manner. This phenomenon may reflect differing signaling or cellular energy demands. In epithelial cells lining the colon, NKA is found in the basolateral membrane and its principle functions include ensuring vectorial Na^+ absorption and generating the driving force for the activity of adjacent electrolyte transporters and ion channels (27). In sperm, NKA can be found in the mid-piece and/or principle piece of the flagellar tail. This places the pump in close proximity to the ATP generating mitochondria that spiral around the axoneme in the mid-piece, and the cohort of ion channels that drive motility (16, 17, 28, 29). Another place where NKA is in close proximity to mitochondria is in photoreceptors. NKA is restricted to

the inner segment plasma membrane adjacent to the bulk of the mitochondria which are clustered in an apical region of the inner segment known as the ellipsoid. In light, the major source of energy consumption is the ciliary outer segment housing the phototransduction cascade. But in the dark, neurotransmitter release from the synaptic terminal and the activity of NKA in the inner segment are the major consumers of energy (30). The close proximity of NKA to the bulk of the mitochondria would seemingly limit the amount of ATP available to the synapse, but this potential problem is minimized by having some of the energy flow from the inner segment to the synapse in the form of phosphocreatine (31). These examples of NKA differential subcellular localization lead one to ask what controls the trafficking of NKA in different cell types.

What is known about the trafficking of NKA relates primarily to early events in the endomembrane system or tethering of the pump in the plasma membrane. For instance, processing through the ER requires assembly of the αβ heterodimer (32–34). This is a common theme among integral membrane proteins, where improper assembly of catalytic and accessory subunits serves as a checkpoint preventing efficient ER exit. Another protein implicated in the trafficking of NKA is ankyrin, an adaptor between membrane proteins and the spectrin-based membrane cytoskeleton (35–37). There are three ankyrin proteins, AnkR, AnkB, and AnkG. In epithelial cells, a two-step model has been proposed whereby AnkR guides the ER to Golgi trafficking of NKA (by binding directly to α1), then AnkG takes over and guides NKA α1 from the Golgi to the plasma membrane (38). Once at adherens junctions in the lateral membrane, NKA is tethered in place in a manner dependent on glycosylation of the β1 subunit (39). At the junctional membranes of T-tubules found in mature cardiomyocytes, AnkB organizes a signaling complex that includes NKA α1 and α2 (40, 41). In the brain, an interaction with AnkB and other components of the membrane cytoskeleton may again come into play to tether NKA α2 or α3 in a Ca^{2+} signaling microdomain known as the junctional ER (42), but see (41). In the retina, AnkB has been proposed to regulate the expression and possibly the trafficking of NKA (43). Other mechanisms to control the trafficking of NKA are unknown and knowledge of how different NKA isozymes may be processed in different cell types is lacking.

We sought to begin addressing this problem by evaluating AnkB as a candidate for regulating the localization of NKA in photoreceptors. In the retina as a whole there is an interaction between NKA and AnkB with the most striking colocalization in the synaptic layers of the inner retina. In photoreceptors, NKA is restricted to the plasma membrane of the inner segment but AnkB did not colocalize in that subdomain of the plasma membrane. Therefore, we turned to examining the subcellular localization of different NKA α subunits expressed in *Xenopus laevis* photoreceptors, a model system previously used in numerous protein trafficking studies (44). We found that NKA α3 localized properly to the plasma membrane of the inner segment when overexpressed in transgenic *Xenopus* photoreceptors while NKA α4 localized to outer segments, a ciliary organelle structurally similar to the flagella where α4 is normally expressed. Analysis of a series of α3/α4 chimeras and mutants revealed a VxP motif within amino acids 1-14 of NKA α4 necessary for localizing the protein to outer segments. This work expands the repertoire of potential mechanisms contributing to differential subcellular localization of NKA isozymes.

RESULTS

Multiple NKA isozymes consisting of α1, α2, or α3 dimerized with β1, β2, or β3 are expressed throughout the retina. Photoreceptors express α3β2 and α3β3 and the localization of these transporters is restricted to the plasma membrane of the inner segment (IS) (45). To identify factors controlling the localization of NKA in photoreceptors, we began by testing for an interaction between NKA and AnkB as they have been previously reported to co-localize along the plasma membrane of the photoreceptor inner segment (43, 46). We found that NKA was co-immunoprecipitated with anti-AnkB antibodies; but the reciprocal experiment did not demonstrate pull down of AnkB with anti-NKA antibodies (Fig 1A). Next, we separated the retina into soluble and membrane protein fractions. The soluble fraction was enriched in actin and GAPDH, while the membrane fraction retained NKA and HCN1, an ion channel expressed throughout the retina. AnkB was greatly enriched in the soluble fraction. Given that AnkB is a component of the membrane cytoskeleton it is surprising that the lysis conditions used here (and in the IP experiments), resulted in the apparent differential extraction of AnkB and NKA (Fig 1B). This observation prompted us to revisit the immunostaining of AnkB and NKA in bovine retina. Using an antibody against NKA that detects all the alpha subunits, robust labeling of the plasma membrane in photoreceptor IS was seen. Labeling was also present in the lower sublamina of the OPL where horizontal, bipolar and Muller glial processes reside. NKA was evenly distributed throughout the inner retina (INL and IPL) as well as the nerve fiber layer. AnkB robustly labeled the OPL, sublamina 1, 3, and 5 of the IPL, and the nerve fiber layer (Fig 1C). These morphologically distinct sublaminae of the IPL represent synaptic connections between different subtypes of bipolar, amacrine, and ganglion cells (47, 48). Surprisingly, immunostaining for AnkB in photoreceptor IS was present but very weak.

An approach to surveying for protein expression across different retinal layers independent of immunohistochemistry is serial tangential sectioning followed by Western blotting (49–51). Using sections collected through mouse retina, NKA and AnkB were found in the same sections, including those representing photoreceptor IS, synapses and inner retinal neurons (Fig 2A). Sections representing the IS and OPL layers were selected based on the distribution of protein markers (i.e. sections 4 and 9 in Fig 2A). The densities of NKA and AnkB bands from those sections were quantified and expressed as the NKA: AnkB ratio, which was 10–20 fold higher in the sections containing photoreceptor IS versus synapses (20.2 ± 11.3 versus 1.1 ± 0.1, respectively). These data do not support NKA localization in the IS via a stoichiometric interaction with AnkB.

Furthermore, immunostaining for AnkB in mouse retina generated a pattern similar to that in the bovine retina. The highest intensity signals originated from the synaptic layers, followed by staining around the photoreceptor nuclei, along the outer limiting membrane and in a faint diffuse pattern within the IS layer. NKA co-localized with AnkB in the synaptic layers (Fig 2B). At higher magnification, colocalization of NKA and AnkB in photoreceptor IS was not apparent (Fig 2C). However, AnkB did co-localize with CRALBP, a Muller glial cell marker, along the outer limiting membrane and in the IS layer (Fig 2D). We conclude that AnkB is expressed in Muller glia and that this could confound the interpretation of immunostained retinas since Muller glia and photoreceptors are densely packed.

In order to visualize the subcellular localization of NKA and AnkB in individual retinal cell types, mouse retinas were dissociated with a combination of gentle mechanical agitation and papain digestion (52–54). The resulting isolated cell fragments were immunostained for NKA and AnkB and identified by morphological criteria. With this procedure we obtained photoreceptor fragments consisting of the myoid portion of the IS still attached to the nucleus (Fig 3A–C) that labeled for both NKA along the membrane and AnkB in the interior of the cell. This difference in subcellular localization of NKA and AnkB is more clearly seen in line scans, where the normalized intensity for each channel along the length of lines drawn perpendicular to the long axis of the myoid is plotted (Fig 3D). AnkB signals were detected throughout the fragments of Muller cells that were obtained, but NKA staining was not detected (Fig 3E–G). Note, the Muller glia span the retina from the microvilli interdigitated around photoreceptor inner segments to the inner limiting membrane separating the retina from the vitreous. Since the fragments do not encompass the entirety of the cell, NKA in Muller glia may be localized to a subcellular domain not released in this dissociation protocol. In neurons with bipolar morphology, AnkB and NKA labeling varied according to subcellular domain. NKA labeled the periphery of the cell consistent with its residence in the plasma membrane, although it was largely absent from synaptic terminals. AnkB labeled the interior of the cell from dendrites to the axon with a strikingly robust signal filling the entire synaptic terminal (Fig 3H–J).

In conclusion, NKA and AnkB are both expressed in diverse cell populations within the retina. But co-localization varies depending on the cell type or subcellular compartment. In intact photoreceptors, NKA is restricted to the IS plasma membrane, while AnkB labeling is more prominent in the adjacent Muller glia microvilli. We cannot rule out that there is additional AnkB in the photoreceptor IS that does co-localize with NKA, but if so, the epitope must be masked for both the monoclonal and polyclonal antibodies that we tested using a variety of fixation conditions (data not shown). For the next phase of this study, we turned to an independent assay to search for trafficking motifs within NKA that contribute to its unique localization pattern in photoreceptors.

The frog retina is a valuable model system for investigating protein localization in photoreceptors due to the large size of the cells and the established protocols for rapidly generating transgenic animals. Immunohistochemistry was used to verify that the expression of NKA in photoreceptor inner segments and inner retina synaptic layers is the same between amphibian and mammalian retinas (Fig 4A, B). Note that *X. laevis* photoreceptors have numerous calycal processes that, depending on the plane of section, may appear to be the plasma membrane at the outer segment base. However, these are microvillus structures which are continuous with the plasma membrane of the inner segment and as such they contain NKA. To determine if the unique concentration of NKA in photoreceptor inner segments is determined by one or more features in the alpha subunit, we expressed several N-terminally GFP-tagged NKA alpha subunits in transgenic *X. laevis* rods (Fig 4, Supplemental Fig 1). A summary of all the constructs presented in this paper is provided (Fig 9). The *X. laevis* sequences of NKA α1 and α3 were used but α4 is specifically expressed in mammalian testes so we used the human sequence. GFP-NKA α3 localized to the IS plasma membrane (ISPM). Since this is where endogenous NKA is found, we

conclude that the placement of the GFP tag did not grossly interfere with targeting of the protein (Fig 4C). Exogenous expression of GFP-NKA α1 also resulted in ISPM localization (Fig 4D). The localization of GFP-NKA α4 differed. It was expressed at particularly low levels but found in a punctate pattern within the outer segments (OS) (Fig 4E). This suggested that in photoreceptors sequence-specific information *dictates* differential localization of NKA α3 and α4.

NKA alpha subunits are highly conserved; α4 is the most divergent yet is still 76% identical to α3. The transmembrane domain core and catalytic domains are the most similar whereas the cytoplasmic N-terminus is less conserved (Supplemental Fig 2B–C). Therefore, we constructed chimeric proteins in which the N-terminus of α3 and α4 were switched and assessed their subcellular localization in transgenic *X. laevis* rods. GFP-α3 (1-82)/α4 was found in the ISPM (Fig 5A), whereas GFP-α4 (1-88)/α3 was found in the OS membranes (Fig 5B). Many protein trafficking determinants are linear motifs within intrinsically disordered regions (55, 56). While crystal structures of NKA α1 are available, they do not include the entire N-terminus (57). Therefore, we analyzed this region of NKA α3 and α4 using meta Protein DisOrder prediction System (58) which revealed that only the first ~40 amino acids of NKA are intrinsically disordered (Supplemental Fig 2D). To test if this region is involved in setting the differential localization, a set of chimeras with this region exchanged were analyzed. GFP-α3 (1-38)/α4 and GFP-α4 (1-44)/α3, were localized in patterns opposite to that of the parent constructs demonstrating that the targeting information lies within the intrinsically disordered region (Fig 6A–B). A subsequent pair of chimeras with only 24 amino acids substituted, GFP-α3 (1-24)/α4 and GFP-α4 (1-24)/α3, was generated and found to also have reversed localization patterns compared to the parent constructs (Fig 6C–D). A final pair of chimeras, GFP-α3 (1-14)/α4 and GFP-α4 (1-14)/α3, revealed that the amino acid motif responsible for differential localization was contained within the first 14 amino acids (Fig 6E–F).

From the chimeric proteins described above, it is not possible to determine if exchanging amino acids 1-14 resulted in a loss-of-inner segment or gain-of-OS targeting. To address this point we used deletion constructs. Deleting the first 14 amino acids from GFP-NKA α3 did not alter its ISPM localization (Fig 7A). However, deleting the corresponding region from GFP-NKA α4 resulted in ISPM localization, indicating that this region contains a gain-of-OS targeting motif (Fig 7B). To pinpoint this motif, we examined sequence alignments of NKA α3 and α4 for residues or patterns unique to α4. Curiously, NKA α4 includes a sequence reminiscent of rhodopsin's C-terminal VxPx ciliary targeting motif (59) (Fig 8A). We made point mutants of those residues and found that GFP-α4 V10A, P12A lost OS localization (Fig 8B). Mutating either valine or proline individually also disrupted OS localization (Fig 8C,D). NKA α3 contains a valine in the same relative position as NKA α4 V10 but not a proline. Mutation of NKA α3 T13P to introduce a "VxP" motif was insufficient to change the localization of GFP-NKA α3 from the ISPM (Fig 8E). This finding, along with the observation that the GFP-NKA α4 (1-14)/α3 chimera (Fig 4E) was the only chimera to have any detectable localization to the ISPM suggested that something within amino acids 15-24 has a secondary influence on trafficking of NKA. NKA α4 contains a series of regularly spaced prolines (P12, P17, P21) in this region which we

hypothesized could influence the function of the VxP motif. GFP-NKA α4 P17A, P21A localized to the OS, indicating that those amino acids are not necessary (Fig 8F). Note, this construct is partially localized in the interior of the IS. Another possible explanation for the insufficiency of adding a VxP to NKA α3 is that the VxP motif is countered by the action of ISPM targeting information elsewhere in NKA α3. We tested if such information might be within residues 15-24 or the entire first 44 amino acids of NKA α3 by deleting those blocks of amino acids. In either case, ISPM targeting remained intact (Fig 8G–H).

Altogether, this series of experiments reveals information regarding two different aspects of NKA trafficking. First, a VxP motif in NKA α4, not present in NKA α3, is minimally necessary for targeting to a ciliary organelle but there is additional sequence and/or structural information within the first 24 amino acids of NKA α4 that influences its activity. Secondly, there is one or more “ISPM targeting” motifs shared by both NKA α3 and NKA α4 downstream of amino acid 44, in the more highly conserved regions of these proteins.

DISCUSSION

There are two main findings coming from this study. The first is that within the retina the colocalization of NKA and ankyrin B varies in a cell type and subcellular domain-dependent manner. Our results indicated that ankyrin is unlikely to play a role in the trafficking of NKA specifically in photoreceptors. Second, we found a VxP motif in the α4 subunit of human NKA that directs its localization to outer segments when expressed in photoreceptors. We propose that this reveals an aspect of the normal targeting of NKA α4 in sperm flagella because both sperm flagella and photoreceptor outer segments are ciliary organelles. Altogether, this work emphasizes the concept that there are multiple mechanisms used differently in specific cell types to control the subcellular localization of NKA isozymes.

In some cell types, ankyrin plays a prominent role in the localization of NKA. Ankyrin (R, B, and G) are large proteins with multiple isoforms and many protein binding partners. They function as adaptors between the spectrin based membrane cytoskeleton and a large number of diverse membrane receptors, ion channels, and adhesion molecules (60, 61). Binding between ankyrin and NKA was first shown in kidney epithelial cells (37). NKA and AnkB specifically, are most clearly associated in ventricular cardiomyocytes where NKA in the T-tubule is part of a Ca^{2+} signaling complex used to regulate contraction. Contraction requires the activation of L-type voltage gated Ca^{2+} channels in the sarcolemma which trigger Ca^{2+} release from the sarcoplasmic reticulum. In order for the muscle to relax, the Ca^{2+} must be cleared and this is handled by the Ca^{2+} pump, SERCA2, and the Na^{+}/Ca^{2+} exchanger, NCX1. AnkB is an organizer of this complex, tethering NKA in close proximity to NCX1 to maintain the high extracellular Na^{+} concentration in this microdomain that is required for the exchanger to function. Both NCX1 and NKA are absent from the T-tubule with reduced expression of AnkB (62). In the brain, a similar role for AnkB organizing NKA and NCX1 at junctional membranes has been debated (41, 42).

In photoreceptors, previous reports demonstrated co-localization of NKA and AnkB along the plasma membrane of the inner segment and throughout the synaptic layers (43, 46).

Here, using two different commercially available antibodies, we also detect AnkB in multiple synaptic layers of the retina and in Muller glial cells, but not along the plasma membrane of the photoreceptor inner segment. We used different antibodies to detect AnkB compared to the previous studies. Therefore, the discrepancy could be explained if the epitopes for the antibodies used here are masked in AnkB localized along the photoreceptor inner segment plasma membrane. Alternatively, it is possible that a specific splice isoform of AnkB only detectable with the antibody used in the previous studies co-localizes with NKA in photoreceptors. To resolve this conundrum, a thorough characterization of the AnkB splice isoforms expressed in the various retinal cells would be very helpful. The recent demonstration that Drop-seq, a method for obtaining single-cell transcriptomes, can be used to identify different cell types in the mouse retina provides encouragement that such information will soon be available (63).

The consistent, robust, labeling of retinal synapses with anti-AnkB antibodies is striking (this study and (43, 46)). AnkB labeling is present in both the OPL (site of synaptic contacts between photoreceptors, bipolar cells, and horizontal cells) and in the IPL (site of synaptic contacts between bipolar, amacrine and ganglion cells). Within the IPL, AnkB labeling was seen in multiple sublaminae such that it could be present in both ON and OFF bipolar cells, including types 1, 2, 5a, 5b, 9 and/or rod bipolar cells (47). This is supported by the observation of AnkB labeling of synapses in isolated retinal neurons with bipolar morphology. Ankyrin is known to participate in synaptic biology, though its exact roles there are still being elucidated. In the *Drosophila* neuromuscular junction, it has been demonstrated that a giant ankyrin is required for both synaptic assembly and stability (64–66). In cultured mammalian neuronal cells, $G_{\alpha o}$ stimulated neurite formation is dependent on the presence of AnkB and AnkG (66). Furthermore, variations in AnkG are linked to psychiatric disorders and recently AnkG has been found to have a dynamic role in shaping dendritic spines in addition to its more well-known role in clustering voltage-dependent sodium channels at the axon initial segment (61, 67). Future studies will hopefully elucidate the contributions synaptic ankyrins make to vision.

In order to find new clues about the trafficking of NKA we turned to a model system that has been particularly fruitful in elucidating various aspects of protein targeting. *Xenopus laevis* tadpoles offer several advantages for studying protein targeting, including large photoreceptors that are straightforward to image, ease of generating transgenic animals, and rapid development. We first confirmed that GFP-tagged NKA α3 localized correctly when over-expressed in rod photoreceptors under the control of the strong XOP promoter. GFP-NKA α3 localized as expected to the ISPM and since trafficking to the plasma membrane in other cells is known to be dependent on the formation of an NKAαβ heterodimer, this indicates that the GFP-tagged α efficiently co-opted endogenous β subunit. The only difference between the endogenous NKA and GFP-NKA α3 was that GFP-NKA α3 was additionally detected throughout the plasma membrane of the synapse. This may be a consequence of overexpressing NKA. GFP-NKA α1 localized as did α3 consistent with their high degree of identity. In contrast, GFP-NKA α4 exogenously expressed in photoreceptors localized to the ciliary outer segment. There, its appearance was remarkably punctate; often giving the outer segments a damaged appearance even though they were

intact at the light level. Possibilities for this phenomenon include that the GFP-NKA α4 formed aggregates, was concentrated into the disc rims, or was in fact damaging to the OS membrane as its catalytic functions were presumably intact. Regardless, this observation provided the opportunity to search for trafficking motifs by analyzing the targeting behavior of chimeric α subunits. With this strategy we determined that a VxP motif in the disordered N-terminus of NKA α4 was necessary, though not sufficient, for outer segment localization.

The VxP motif in NKA α4 is similar to other ciliary targeting motifs, notably the C-terminal VxPx motif in rhodopsin and the N-terminal RVxP motif in polycystin-2 (59, 68, 69). While photoreceptors can serve as a good model for other ciliary structures, they do have a uniquely elaborated membrane domain which could confound the issue. For instance, many non-targeted membrane proteins accumulate in outer segments when exogenously expressed in photoreceptors. This phenomenon is particularly striking in *X. laevis* rods, where OS targeted and non-targeted localization patterns can appear identical (70). In the smaller OS of mice this is less of a problem since non-targeted membrane proteins are approximately equally distributed throughout the entire cell, including the OS (71). We conclude that the VxP motif in NKA α4 is necessary for active targeting to this ciliary compartment because the constructs with the VxP motif absent were found exclusively in the ISPM which would not be the case if they had simply become non-targeted. The VxP motif in human NKA α4 is remarkably conserved across the majority of mammalian species (Supplemental Figure 3). But it is not invariant. This is most notable in the rodents, though many just have an extra amino acid separating the critical valine and proline (VxxP vs. VxP). Given that this is an intrinsically disordered region, this spacing difference is unlikely to have a large impact on subcellular targeting. Ultimately, verification of the contribution that the VxP motif makes in flagellar targeting of NKA α4 will be challenging as there is little to no active transcription or translation in sperm (72). The best way to test the necessity of the VxP motif in sperm may be to replicate some of the experiments presented here using transgenic mice.

In conclusion, we predict that the identification of the VxP-dependent outer segment targeting of NKA α4 reflects a mechanism at play in sperm flagella where NKA α4 is endogenously expressed. This is just the tip of the iceberg when it comes to unraveling the mechanisms controlling the differential subcellular localization of the various NKA isoforms in all the cell types in which they are expressed, with this finding as an important initial step.

MATERIALS AND METHODS

Protein Biology

Frozen bovine retinas (Lawson) were homogenized in IP buffer (50 mM Tris, pH 7.3, 10 mM NaCl, 0.32 M sucrose, 5 mM EDTA, 2.5 M EGTA, 1 mM PMSF) supplemented with protease inhibitor cocktail (Complete, Roche) and clarify by centrifugation at 1,000 × g for 10 minutes. Immunoprecipitations were carried out with 1 mg of lysate and 5 μg of either mouse α-NKA (M7-PB-E9, Santa Cruz), mouse α-NKA α3 (XVIF9-G10, Thermo Scientific), mouse α-Ankyrin B (clone N105/13, NeuroMab), or mouse IgG (Sigma) incubated with 1.5 mg Protein G Dynabeads (Life Technologies) for 2 hour. The beads were washed in PBS and eluted in LDS sample buffer. IP with each precipitating antibody were

replicated at least twice. For retina fractionation experiments the retinas were depleted of photoreceptor outer segments by gentle shaking in Buffer A (50% sucrose, 10mM HEPES, pH7.4, 1mM EDTA, 5mM $MgCl_2$) supplemented with protease inhibitor cocktail. After centrifugation at 13,000 × g, 1hr the pelleted retina was resuspended in Buffer A without sucrose. A centrifugation step at 750 × g for 10 min was used to clarify the lysate. The "total" lysate was then centrifuged at 100,000 × g for 1h to separate soluble proteins from membranes and 20 μg of total protein from each fraction were analyzed by Western blotting. Serial tangential sectioning of mouse retinas followed by Western blotting was performed as previously described (49, 50). Three independent sets of retinal sections were blotted for NKA, AnkB and markers for photoreceptor OS and IS. Antibodies for Western blotting were used as follows: mouse α-NKA (1:1000, M7-PB-E9, Santa Cruz), rabbit α-HCN1 (1:2500,(73)), mouse α-actin (1:1000, AC-74, Sigma), rabbit α-GAPDH (1:250, Abcam), mouse α-Ankyrin B (1:1000, clone N105/13, NeuroMab), rabbit α-rod transducin, $T_{\alpha 1}$ (K-20, Santa Cruz), rabbit α-arrestin (PA1-731, Thermo Fisher), and α-Rom-1 (a gift from Dr Andrew Goldberg).

Molecular Biology

All transgenic constructs were created using standard PCR protocols in order to fuse GFP to the N-terminus of the NKA isoform or mutant, then subcloned into the AgeI and NotI sites of the XOP5.5 vector. This vector contains a *Xenopus* rhodopsin promoter used to drive rod photoreceptor specific expression (74). Constructs were verified with Sanger sequencing (Iowa Institute of Human Genetics, University of Iowa). Sequences of plasmid inserts and primers are available on request. The cDNAs used as templates for cloning the various constructs included *Xenopus laevis* ATP1a3 (BC043743), *Xenopus laevis* ATP1a1 (NP_989407.1), and *Homo sapiens* ATP1a4 (BC094801) were all purchased from Open Biosystems.

Animals and Transgenesis

Mice (C57/Bl6J) were obtained from The Jackson Laboratories. Adult *Xenopus laevis* were obtained from Nasco and maintained by the Office of Animal Research at the University of Iowa. All experiments were approved by the Institutional Animal Care and Use Committee and adhered to the ARVO guidelines for animal use in vision research. Transgenic *Xenopus* tadpoles were generated using restriction enzyme mediated integration (REMI) as previously described (75). Briefly, egg laying was stimulated with injections into the dorsal lymph sac of 200U of pregnant mare serum gonadotropin followed 3–5 days later by 500U of human chorionic gonadotropin (Prospect). Transgenic nuclei generated using the REMI reaction were transplanted into dejellied eggs maintained in 6% Ficoll, 0.4x Marc's Modified Ringer (MMR) (1x MMR is 100 mM NaCl, 2 mM KCL, 1 mM $MgCl_2$, 2 mM $CaCl_2$, 5 mM HEPES, pH 7.4) through Stage 7. Embryos were switched to 4% Ficoll, 0.3x MMR then maintained in 0.3x MMR post-gastrulation. At St 42 transgenic tadpoles were identified by screening for GFP expression in the eye and then transitioned into 0.1% Instant Ocean sea salt. Tadpoles were humanely euthanized between St 45 and 55 by immersion in 0.2% tricaine prior to processing for immunohistochemistry.

Immunohistochemistry

Transgenic tadpoles were fixed in 4% paraformaldehyde (Electron Microscopy Sciences) in Frog Ringer (115 mM NaCl, 2 mM KCl, 1 mM $CaCl_2$, 1 mM $MgCl_2$, 5 mM HEPES, pH 7.4) for 45 min, cryoprotected in 30% sucrose, and frozen in Tissue-Tek O.C.T (Electron Microscopy Sciences). Sections collected on charged glass slides were permeablilized in 0.5% Triton X-100, blocked with 5% goat serum and 0.5% Triton X-100 in PBS, incubated in mouse α-GFP antibodies (4C9 supernatant diluted 1:5, Developmental Hybridoma Studies Bank). Tissue sections were incubated in secondary goat α-mouse antibodies conjugated to Alexa 568 (Life Technologies) mixed with 2 μg/mL Hoechst 33342 (Life Technologies) to label the nuclei. Bovine or mouse retina was fixed in 4% paraformaldehyde in PBS for 15 min or 45 min and frozen in OCT. Isolated retinal cell fragments were obtained using the Worthington Papain Dissociation System according to instructions from the manufactor (Worthington Biochemical Corporation). Isolated cell fragments were fixed in 4% paraformaldehyde in PBS for 45 min, and allowed to settle onto a chambered slide overnight at 4°C prior to immunostaining.

The following antibodies were used for immunostaining: mouse α-NKA (1:1000, M7-PB-E9, Santa Cruz), rabbit α-Ankyrin B (1:500, H-300, Santa Cruz), mouse α-Ankyrin B (1:100, clone N105/13, NeuroMab), rabbit α-CRALBP (1:50, H-100, Santa Cruz). Images were collected using a Zeiss 710 confocal microscope (Central Microscopy Research Facility, University of Iowa). Manipulation of images was limited to adjusting the brightness and contrast levels using Zen Light 2009/2012 (Carl Zeiss Microscopy) or Photoshop (Adobe Systems Inc.). A minimum of three individual transgenic tadpoles were studied for every DNA construct.

Supplementary Material

Refer to Web version on PubMed Central for supplementary material.

Acknowledgments

This research was supported by grants from the National Institutes of Health, EY020542 (SAB), EY019665 (MS) and an unrestricted Research to Prevent Blindness Grant awarded to West Virginia University Eye Institute. Preliminary experiments conducted by SAB at Duke University were supported by a National Institutes of Health Core Grant for Vision Research, EY5722, and an unrestricted grant from Research to Prevent Blindness Grant awarded to Duke University. All authors contributed to the design, execution, and analysis of the experiments. JGL and SAB wrote the manuscript.

Abbreviations

NKA	sodium potassium ATPase
OS	outer segment
IS	inner segment
ISPM	inner segment plasma membrane
OLM	outer limiting membrane

ONL	outer nuclear layer
OPL	outer plexiform layer
INL	inner nuclear layer
IPL	inner plexiform layer
GC	ganglion cell layer
NFL	nerve fiber layer
ank	ankyrin
AnkB	ankyrin-B

References

1. Reinhard L, Tidow H, Clausen MJ, Nissen P. Na(+),K (+)-ATPase as a docking station: protein-protein complexes of the Na(+),K (+)-ATPase. Cellular and molecular life sciences : CMLS. 2013; 70(2):205–222. [PubMed: 22695678]
2. Xie JX, Shapiro AP, Shapiro JI. The Trade-Off between Dietary Salt and Cardiovascular Disease; A Role for Na/K-ATPase Signaling? Frontiers in endocrinology. 2014; 5:97. [PubMed: 25101054]
3. Hilgenberg LG, Su H, Gu H, O'Dowd DK, Smith MA. Alpha3Na+/K+-ATPase is a neuronal receptor for agrin. Cell. 2006; 125(2):359–369. [PubMed: 16630822]
4. Vagin O, Dada LA, Tokhtaeva E, Sachs G. The Na-K-ATPase alpha(1)beta(1) heterodimer as a cell adhesion molecule in epithelia. American journal of physiology Cell physiology. 2012; 302(9):C1271–1281. [PubMed: 22277755]
5. Friedrich U, Stohr H, Hilfinger D, Loenhardt T, Schachner M, Langmann T, Weber BH. The Na/K-ATPase is obligatory for membrane anchorage of retinoschisin, the protein involved in the pathogenesis of X-linked juvenile retinoschisis. Hum Mol Genet. 2011; 20(6):1132–1142. [PubMed: 21196491]
6. Molday LL, Wu WW, Molday RS. Retinoschisin (RS1), the protein encoded by the X-linked retinoschisis gene, is anchored to the surface of retinal photoreceptor and bipolar cells through its interactions with a Na/K ATPase-SARM1 complex. The Journal of biological chemistry. 2007; 282(45):32792–32801. [PubMed: 17804407]
7. Molday RS, Kellner U, Weber BH. X-linked juvenile retinoschisis: clinical diagnosis, genetic analysis, and molecular mechanisms. Progress in retinal and eye research. 2012; 31(3):195–212. [PubMed: 22245536]
8. James PF, Grupp IL, Grupp G, Woo AL, Askew GR, Croyle ML, Walsh RA, Lingrel JB. Identification of a specific role for the Na,K-ATPase alpha 2 isoform as a regulator of calcium in the heart. Molecular cell. 1999; 3(5):555–563. [PubMed: 10360172]
9. Beuschlein F, Boulkroun S, Osswald A, Wieland T, Nielsen HN, Lichtenauer UD, Penton D, Schack VR, Amar L, Fischer E, Walther A, Tauber P, Schwarzmayr T, Diener S, Graf E, et al. Somatic mutations in ATP1A1 and ATP2B3 lead to aldosterone-producing adenomas and secondary hypertension. Nature genetics. 2013; 45(4):440–444. 444e441–442. [PubMed: 23416519]
10. Williams TA, Monticone S, Schack VR, Stindl J, Burrello J, Buffolo F, Annaratone L, Castellano I, Beuschlein F, Reincke M, Lucatello B, Ronconi V, Fallo F, Bernini G, Maccario M, et al. Somatic ATP1A1, ATP2B3, and KCNJ5 mutations in aldosterone-producing adenomas. Hypertension. 2014; 63(1):188–195. [PubMed: 24082052]
11. Azizan EA, Poulsen H, Tuluc P, Zhou J, Clausen MV, Lieb A, Maniero C, Garg S, Bochukova EG, Zhao W, Shaikh LH, Brighton CA, Teo AE, Davenport AP, Dekkers T, et al. Somatic mutations in ATP1A1 and CACNA1D underlie a common subtype of adrenal hypertension. Nature genetics. 2013; 45(9):1055–1060. [PubMed: 23913004]

12. Gritz SM, Radcliffe RA. Genetic effects of ATP1A2 in familial hemiplegic migraine type II and animal models. Human genomics. 2013; 7:8. [PubMed: 23561701]
13. Heinzen EL, Arzimanoglou A, Brashear A, Clapcote SJ, Gurrieri F, Goldstein DB, Johannesson SH, Mikati MA, Neville B, Nicole S, Ozelius LJ, Poulsen H, Schyns T, Sweadner KJ, van den Maagdenberg A, et al. Distinct neurological disorders with ATP1A3 mutations. The Lancet Neurology. 2014; 13(5):503–514. [PubMed: 24739246]
14. Sweney MT, Newcomb TM, Swoboda KJ. The Expanding Spectrum of Neurological Phenotypes in Children With ATP1A3 Mutations, Alternating Hemiplegia of Childhood, Rapid-onset Dystonia-Parkinsonism, CAPOS and Beyond. Pediatric neurology. 2014
15. Jimenez T, Sanchez G, Wertheimer E, Blanco G. Activity of the Na,K-ATPase alpha4 isoform is important for membrane potential, intracellular Ca2+, and pH to maintain motility in rat spermatozoa. Reproduction (Cambridge, England). 2010; 139(5):835–845.
16. Woo AL, James PF, Lingrel JB. Roles of the Na,K-ATPase alpha4 isoform and the Na+/H+ exchanger in sperm motility. Molecular reproduction and development. 2002; 62(3):348–356. [PubMed: 12112599]
17. Wagoner K, Sanchez G, Nguyen AN, Enders GC, Blanco G. Different expression and activity of the alpha1 and alpha4 isoforms of the Na,K-ATPase during rat male germ cell ontogeny. Reproduction (Cambridge, England). 2005; 130(5):627–641.
18. Jimenez T, McDermott JP, Sanchez G, Blanco G. Na,K-ATPase alpha4 isoform is essential for sperm fertility. Proc Natl Acad Sci U S A. 2011; 108(2):644–649. [PubMed: 21187400]
19. Aschauer L, Gruber LN, Pfaller W, Limonciel A, Athersuch TJ, Cavill R, Khan A, Gstraunthaler G, Grillari J, Grillari R, Hewitt P, Leonard MO, Wilmes A, Jennings P. Delineation of the key aspects in the regulation of epithelial monolayer formation. Molecular and cellular biology. 2013; 33(13):2535–2550. [PubMed: 23608536]
20. Bhavsar SK, Hosseinzadeh Z, Brenner D, Honisch S, Jilani K, Liu G, Szteyn K, Sopjani M, Mak TW, Shumilina E, Lang F. Energy-sensitive regulation of Na+/K+-ATPase by Janus kinase 2. American journal of physiology Cell physiology. 2014; 306(4):C374–384. [PubMed: 24304834]
21. Herman MB, Rajkhowa T, Cutuli F, Springate JE, Taub M. Regulation of renal proximal tubule Na-K-ATPase by prostaglandins. American journal of physiology Renal physiology. 2010; 298(5):F1222–1234. [PubMed: 20130120]
22. Johar K, Priya A, Wong-Riley MT. Regulation of Na(+)/K(+)-ATPase by nuclear respiratory factor 1: implication in the tight coupling of neuronal activity, energy generation, and energy consumption. The Journal of biological chemistry. 2012; 287(48):40381–40390. [PubMed: 23048038]
23. Johar K, Priya A, Wong-Riley MT. Regulation of Na(+)/K(+)-ATPase by neuron-specific transcription factor Sp4: implication in the tight coupling of energy production, neuronal activity and energy consumption in neurons. Eur J Neurosci. 2014; 39(4):566–578. [PubMed: 24219545]
24. Wang G, Kawakami K, Gick G. Regulation of Na,K-ATPase alpha1 subunit gene transcription in response to low K(+): role of CRE/ATF- and GC box-binding proteins. J Cell Physiol. 2007; 213(1):167–176. [PubMed: 17477345]
25. Watanabe Y, Kawakami K, Hirayama Y, Nagano K. Transcription factors positively and negatively regulating the Na,K-ATPase alpha 1 subunit gene. Journal of biochemistry. 1993; 114(6):849–855. [PubMed: 8138542]
26. McDermott JP, Sanchez G, Chennathukuzhi V, Blanco G. Green fluorescence protein driven by the Na,K-ATPase alpha4 isoform promoter is expressed only in male germ cells of mouse testis. Journal of assisted reproduction and genetics. 2012; 29(12):1313–1325. [PubMed: 23229519]
27. Bachmann O, Juric M, Seidler U, Manns MP, Yu H. Basolateral ion transporters involved in colonic epithelial electrolyte absorption, anion secretion and cellular homeostasis. Acta physiologica (Oxford, England). 2011; 201(1):33–46.
28. Hlivko JT, Chakraborty S, Hlivko TJ, Sengupta A, James PF. The human Na,K-ATPase alpha 4 isoform is a ouabain-sensitive alpha isoform that is expressed in sperm. Molecular reproduction and development. 2006; 73(1):101–115. [PubMed: 16175638]
29. Miller MR, Mansell SA, Meyers SA, Lishko PV. Flagellar ion channels of sperm: similarities and differences between species. Cell calcium. 2014

30. Okawa H, Sampath AP, Laughlin SB, Fain GL. ATP consumption by mammalian rod photoreceptors in darkness and in light. Current biology : CB. 2008; 18(24):1917–1921. [PubMed: 19084410]

31. Linton JD, Holzhausen LC, Babai N, Song H, Miyagishima KJ, Stearns GW, Lindsay K, Wei J, Chertov AO, Peters TA, Caffe R, Pluk H, Seeliger MW, Tanimoto N, Fong K, et al. Flow of energy in the outer retina in darkness and in light. Proceedings of the National Academy of Sciences of the United States of America. 2010; 107(19):8599–8604. [PubMed: 20445106]

32. Tokhtaeva E, Sachs G, Vagin O. Assembly with the Na,K-ATPase alpha(1) subunit is required for export of beta(1) and beta(2) subunits from the endoplasmic reticulum. Biochemistry. 2009; 48(48):11421–11431. [PubMed: 19764716]

33. Ackermann U, Geering K. Mutual dependence of Na,K-ATPase alpha- and beta-subunits for correct posttranslational processing and intracellular transport. FEBS Lett. 1990; 269(1):105–108. [PubMed: 2167238]

34. Morton MJ, Farr GA, Hull M, Capendeguy O, Horisberger JD, Caplan MJ. Association with {beta}-COP regulates the trafficking of the newly synthesized Na,K-ATPase. The Journal of biological chemistry. 2010; 285(44):33737–33746. [PubMed: 20801885]

35. Devarajan P, Scaramuzzino DA, Morrow JS. Ankyrin binds to two distinct cytoplasmic domains of Na,K-ATPase alpha subunit. Proc Natl Acad Sci U S A. 1994; 91(8):2965–2969. [PubMed: 8159688]

36. Jordan C, Puschel B, Koob R, Drenckhahn D. Identification of a binding motif for ankyrin on the alpha-subunit of Na+,K(+)-ATPase. The Journal of biological chemistry. 1995; 270(50):29971–29975. [PubMed: 8530398]

37. Nelson WJ, Veshnock PJ. Ankyrin binding to (Na+ + K+)ATPase and implications for the organization of membrane domains in polarized cells. Nature. 1987; 328(6130):533–536. [PubMed: 3039371]

38. Stabach PR, Devarajan P, Stankewich MC, Bannykh S, Morrow JS. Ankyrin facilitates intracellular trafficking of alpha1-Na+-K+-ATPase in polarized cells. American journal of physiology Cell physiology. 2008; 295(5):C1202–1214. [PubMed: 18768923]

39. Vagin O, Tokhtaeva E, Sachs G. The role of the beta1 subunit of the Na,K-ATPase and its glycosylation in cell-cell adhesion. The Journal of biological chemistry. 2006; 281(51):39573–39587. [PubMed: 17052981]

40. Kline CF, Scott J, Curran J, Hund TJ, Mohler PJ. Ankyrin-B regulates Cav2.1 and Cav2.2 channel expression and targeting. The Journal of biological chemistry. 2014; 289(8):5285–5295. [PubMed: 24394417]

41. Mohler PJ, Davis JQ, Bennett V. Ankyrin-B coordinates the Na/K ATPase, Na/Ca exchanger, and InsP3 receptor in a cardiac T-tubule/SR microdomain. PLoS biology. 2005; 3(12):e423. [PubMed: 16292983]

42. Lencesova L, O'Neill A, Resneck WG, Bloch RJ, Blaustein MP. Plasma membrane-cytoskeleton-endoplasmic reticulum complexes in neurons and astrocytes. The Journal of biological chemistry. 2004; 279(4):2885–2893. [PubMed: 14593108]

43. Kizhatil K, Sandhu NK, Peachey NS, Bennett V. Ankyrin-B is required for coordinated expression of beta-2-spectrin, the Na/K-ATPase and the Na/Ca exchanger in the inner segment of rod photoreceptors. Exp Eye Res. 2009; 88(1):57–64. [PubMed: 19007774]

44. Pearring JN, Salinas RY, Baker SA, Arshavsky VY. Protein sorting, targeting and trafficking in photoreceptor cells. Progress in retinal and eye research. 2013; 36:24–51. [PubMed: 23562855]

45. Wetzel RK, Arystarkhova E, Sweadner KJ. Cellular and subcellular specification of Na,K-ATPase alpha and beta isoforms in the postnatal development of mouse retina. The Journal of neuroscience : the official journal of the Society for Neuroscience. 1999; 19(22):9878–9889. [PubMed: 10559397]

46. Kizhatil K, Baker SA, Arshavsky VY, Bennett V. Ankyrin-G promotes cyclic nucleotide-gated channel transport to rod photoreceptor sensory cilia. Science. 2009; 323(5921):1614–1617. [PubMed: 19299621]

47. Wassle H, Puller C, Muller F, Haverkamp S. Cone contacts, mosaics, and territories of bipolar cells in the mouse retina. The Journal of neuroscience : the official journal of the Society for Neuroscience. 2009; 29(1):106–117. [PubMed: 19129389]
48. Masland RH. The neuronal organization of the retina. Neuron. 2012; 76(2):266–280. [PubMed: 23083731]
49. Belcastro M, Song H, Sinha S, Song C, Mathers PH, Sokolov M. Phosphorylation of phosducin accelerates rod recovery from transducin translocation. Investigative Ophthalmology and Visual Science. 2012; 53(6):3084–3091. [PubMed: 22491418]
50. Song H, Sokolov M. Analysis of protein expression and compartmentalization in retinal neurons using serial tangential sectioning of the retina. Journal of proteome research. 2009; 8(1):346–351. [PubMed: 19049346]
51. Sokolov M, Lyubarsky AL, Strissel KJ, Savchenko AB, Govardovskii VI, Pugh EN Jr, Arshavsky VY. Massive light-driven translocation of transducin between the two major compartments of rod cells: a novel mechanism of light adaptation. Neuron. 2002; 34(1):95–106. [PubMed: 11931744]
52. Wahlin KJ, Lim L, Grice EA, Campochiaro PA, Zack DJ, Adler R. A method for analysis of gene expression in isolated mouse photoreceptor and Muller cells. Mol Vis. 2004; 10:366–375. [PubMed: 15205663]
53. Feodorova Y, Koch M, Bultman S, Michalakis S, Solovei I. Quick and reliable method for retina dissociation and separation of rod photoreceptor perikarya from adult mice. MethodsX. 2015; 2:39–46. [PubMed: 26150970]
54. Sarthy PV, Bridges CD, Kretzer FL, Lam DM. Lectin receptors on cells isolated from the turtle retina. J Comp Neurol. 1981; 202(4):561–569. [PubMed: 7298915]
55. Dinkel H, Van Roey K, Michael S, Davey NE, Weatheritt RJ, Born D, Speck T, Kruger D, Grebnev G, Kuban M, Strumillo M, Uyar B, Budd A, Altenberg B, Seiler M, et al. The eukaryotic linear motif resource ELM: 10 years and counting. Nucleic acids research. 2014; 42(Database issue):D259–266. [PubMed: 24214962]
56. Stoops EH, Caplan MJ. Trafficking to the apical and basolateral membranes in polarized epithelial cells. Journal of the American Society of Nephrology : JASN. 2014; 25(7):1375–1386. [PubMed: 24652803]
57. Toyoshima C, Kanai R, Cornelius F. First crystal structures of Na+,K+-ATPase: new light on the oldest ion pump. Structure. 2011; 19(12):1732–1738. [PubMed: 22153495]
58. Ishida T, Kinoshita K. Prediction of disordered regions in proteins based on the meta approach. Bioinformatics. 2008; 24(11):1344–1348. [PubMed: 18426805]
59. Tam BM, Moritz OL, Hurd LB, Papermaster DS. Identification of an outer segment targeting signal in the COOH terminus of rhodopsin using transgenic Xenopus laevis. The Journal of cell biology. 2000; 151(7):1369–1380. [PubMed: 11134067]
60. Wang C, Wei Z, Chen K, Ye F, Yu C, Bennett V, Zhang M. Structural basis of diverse membrane target recognitions by ankyrins. eLife. 2014:3.
61. Bennett V, Healy J. Membrane domains based on ankyrin and spectrin associated with cell-cell interactions. Cold Spring Harbor perspectives in biology. 2009; 1(6):a003012. [PubMed: 20457566]
62. Kline CF, Mohler PJ. Evolving form to fit function: cardiomyocyte intercalated disc and transverse-tubule membranes. Current topics in membranes. 2013; 72:121–158. [PubMed: 24210429]
63. Macosko EZ, Basu A, Satija R, Nemesh J, Shekhar K, Goldman M, Tirosh I, Bialas AR, Kamitaki N, Martersteck EM, Trombetta JJ, Weitz DA, Sanes JR, Shalek AK, Regev A, et al. Highly Parallel Genome-wide Expression Profiling of Individual Cells Using Nanoliter Droplets. Cell. 2015; 161(5):1202–1214. [PubMed: 26000488]
64. Pielage J, Cheng L, Fetter RD, Carlton PM, Sedat JW, Davis GW. A presynaptic giant ankyrin stabilizes the NMJ through regulation of presynaptic microtubules and transsynaptic cell adhesion. Neuron. 2008; 58(2):195–209. [PubMed: 18439405]
65. Koch I, Schwarz H, Beuchle D, Goellner B, Langegger M, Aberle H. Drosophila ankyrin 2 is required for synaptic stability. Neuron. 2008; 58(2):210–222. [PubMed: 18439406]

66. Luchtenborg AM, Solis GP, Egger-Adam D, Koval A, Lin C, Blanchard MG, Kellenberger S, Katanaev VL. Heterotrimeric Go protein links Wnt-Frizzled signaling with ankyrins to regulate the neuronal microtubule cytoskeleton. Development. 2014; 141(17):3399–3409. [PubMed: 25139856]

67. Smith KR, Kopeikina KJ, Fawcett-Patel JM, Leaderbrand K, Gao R, Schurmann B, Myczek K, Radulovic J, Swanson GT, Penzes P. Psychiatric Risk Factor ANK3/Ankyrin-G Nanodomains Regulate the Structure and Function of Glutamatergic Synapses. Neuron. 2014; 84(2):399–415. [PubMed: 25374361]

68. Geng L, Okuhara D, Yu Z, Tian X, Cai Y, Shibazaki S, Somlo S. Polycystin-2 traffics to cilia independently of polycystin-1 by using an N-terminal RVxP motif. Journal of cell science. 2006; 119(Pt 7):1383–1395. [PubMed: 16537653]

69. Pazour GJ, Bloodgood RA. Targeting proteins to the ciliary membrane. Curr Top Dev Biol. 2008; 85:115–149. [PubMed: 19147004]

70. Baker SA, Haeri M, Yoo P, Gospe SM 3rd, Skiba NP, Knox BE, Arshavsky VY. The outer segment serves as a default destination for the trafficking of membrane proteins in photoreceptors. The Journal of cell biology. 2008; 183(3):485–498. [PubMed: 18981232]

71. Pearring JN, Lieu EC, Winter JR, Baker SA, Arshavsky VY. R9AP targeting to rod outer segments is independent of rhodopsin and is guided by the SNARE homology domain. Molecular biology of the cell. 2014; 25(17):2644–2649. [PubMed: 25009288]

72. Miller D, Ostermeier GC. Spermatozoal RNA: Why is it there and what does it do? Gynecologie, obstetrique & fertilite. 2006; 34(9):840–846.

73. Pan Y, Bhattarai S, Modestou M, Drack AV, Chetkovich DM, Baker SA. TRIP8b is required for maximal expression of HCN1 in the mouse retina. PloS one. 2014; 9(1):e85850. [PubMed: 24409334]

74. Knox BE, Schlueter C, Sanger BM, Green CB, Besharse JC. Transgene expression in Xenopus rods. FEBS Lett. 1998; 423(2):117–121. [PubMed: 9512341]

75. Pan Y, Laird JG, Yamaguchi DM, Baker SA. A diarginine ER retention signal regulates trafficking of HCN1 channels from the early secretory pathway to the plasma membrane. Cellular and molecular life sciences : CMLS. 2015; 72:833–843. [PubMed: 25142030]

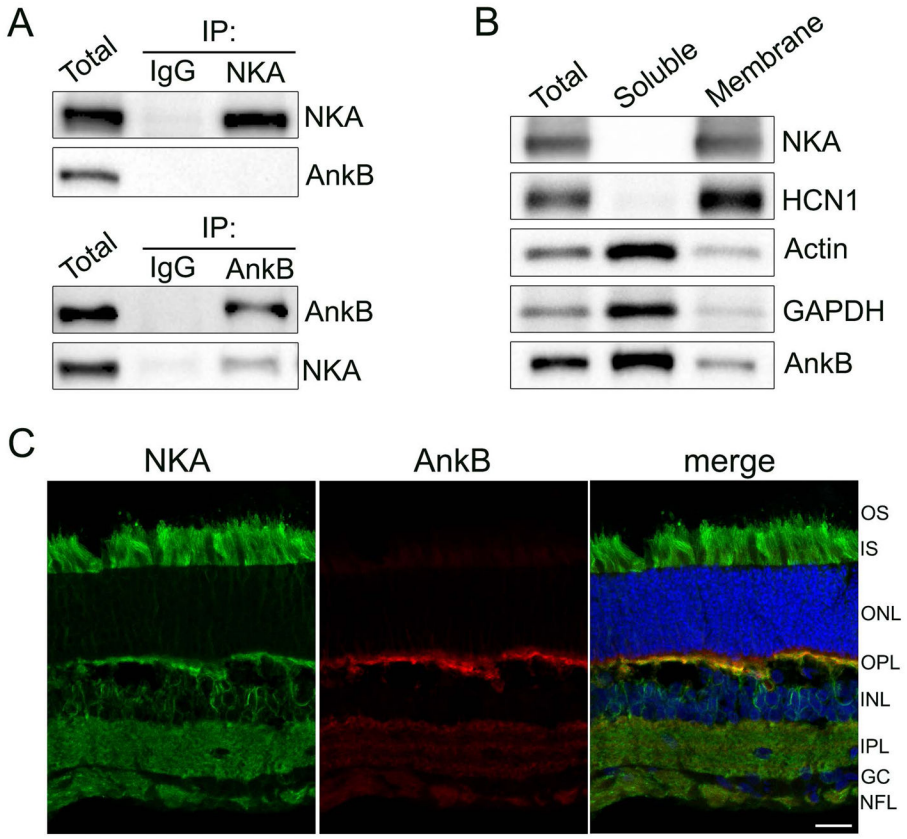

Figure 1. NKA and AnkB in bovine retina

A) Co-immunoprecipitations from bovine retinal lysates, blotted for NKA and AnkB. Either anti-NKA antibodies (upper panel) or anti-AnkB antibodies (lower panel) alongside IgG as a negative control were used as the precipitating antibodies. *B*) Bovine retina, after depletion of photoreceptor outer segments and nuclei, separated into soluble versus membrane fractions. Membrane fraction verified by blotting for NKA and HCN1, soluble fraction verified by blotting for actin and GAPDH. AnkB was enriched in the soluble fraction. *C*) Double labeling of bovine retina with antibodies against NKA (green) and AnkB (red). Scale bar is 20 μm and nuclei labeled with Hoechst in merged images in C and D. Abbreviations: OS, outer segment; IS, inner segment; ONL, outer nuclear layer; OPL, outer plexiform layer; INL, inner nuclear layer; IPL, inner plexiform layer; GC, ganglion cell layer; NFL, nerve fiber layer.

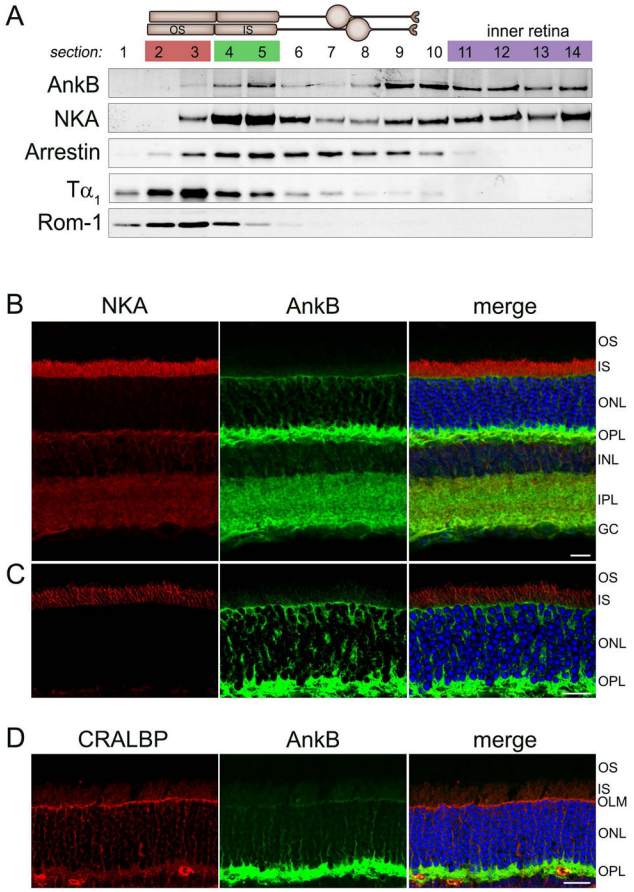

Figure 2. NKA and AnkB localization in mouse retina

A) Serial tangential sections through a dark-adapted mouse retina blotted for AnkB, NKA, arrestin (marker for photoreceptor IS, soma, and synapse), transducin alpha (Tα) (marker for OS) and Rom-1 (marker for OS). AnkB and NKA are present in the same sections throughout the retina. *B, C)* Double labeling of mouse retina with antibodies against NKA (red) and AnkB (green) or *D)* CRALBP (red) and AnkB (green). Scale bar is 20 μm (B–D), abbreviations as in Fig 1; OLM is outer limiting membrane, the band of adherens junctions between Muller glia and photoreceptor inner segments.

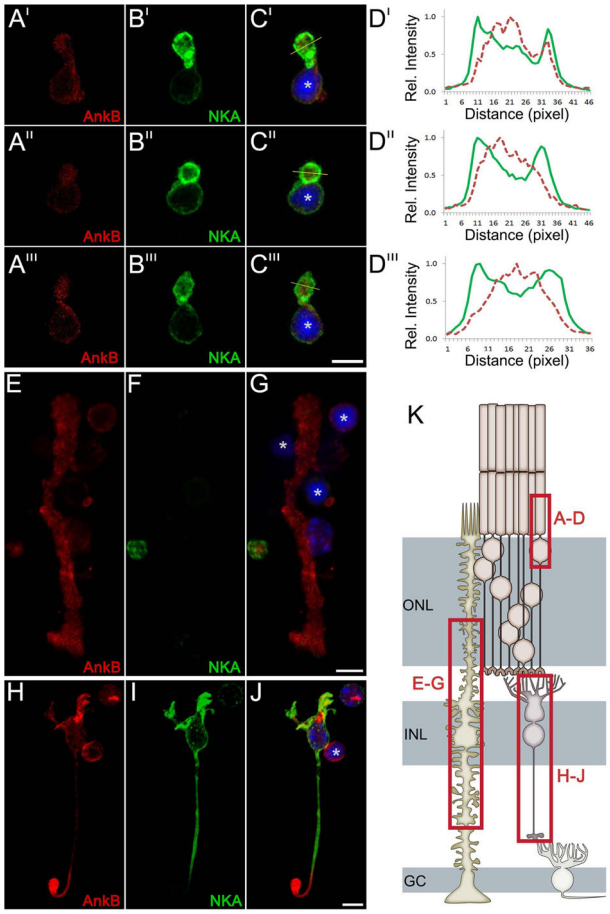

Figure 3. NKA and AnkB localization in dissociated mouse retina cell fragments

Immunostaining for AnkB (red) and NKA (green) in cellular fragments identified by morphology. The schematic in *(K)* places the images of the cell fragments shown in (A–J) in context of their original location in intact retina. *A^{I-III}–C^{I-III})* Three examples of isolated photoreceptor inner segments (myoid) attached to the soma containing the nucleus. AnkB labeling is interior to the NKA labeling, as seen in the merged images (*C^{I-III})* and line scan plots (*D^{I-III})* where the normalized signal intensity of AnkB (red, dashed line) and NKA (green, solid line) along the length of lines arbitrarily drawn perpendicular to the long axis of the photoreceptor myoid (yellow lines in C^{I-III}) is plotted. *E–G)* Fragment of a Muller glial cell; identified by the thick diameter, length, and numerous small processes. AnkB labeled the entirety of this fragment, but NKA was not detected. Asterisk indicates isolated nuclei from broken rod photoreceptors identified by the unique central condensation of heterochromatin *(C,G,J). H–J)* Bipolar neuron as identified by tufts of dendrites adjacent to the nucleus, long axon and large synapse. AnkB labeling is interior to the NKA labeling in the dendrites, soma, and axon; AnkB but not NKA was enriched in the synaptic terminal. Scale bar is 5 μm for each set of panels.

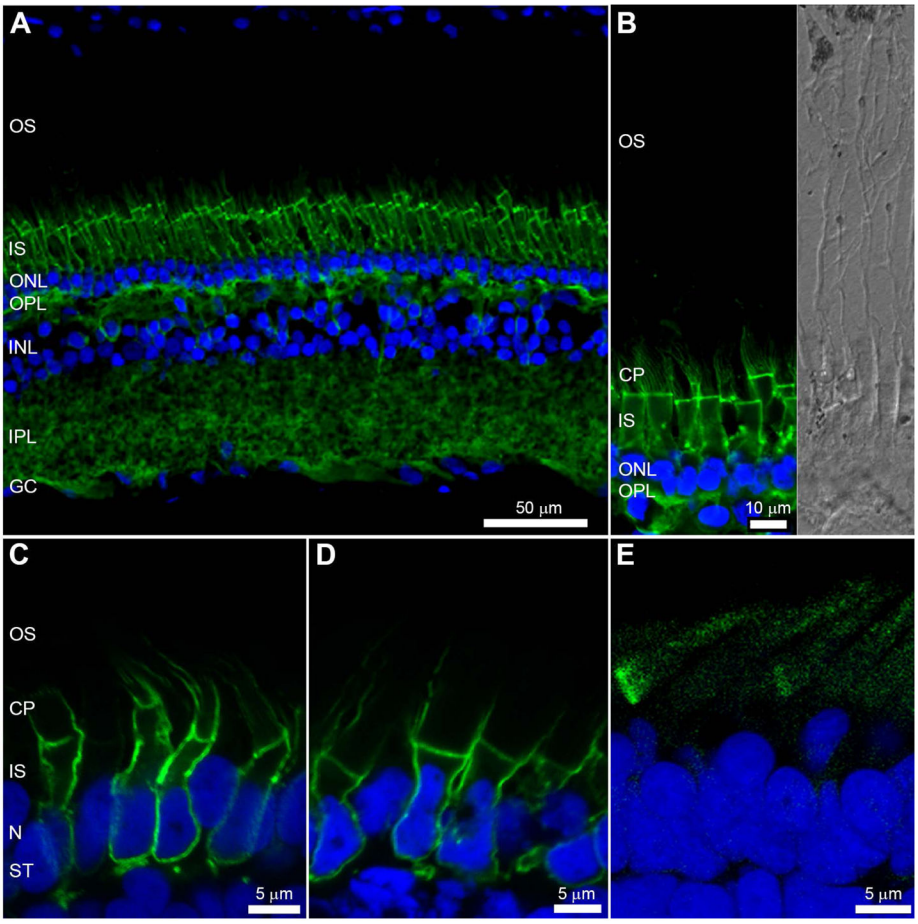

Figure 4. Expression of NKA in *X. laevis* photoreceptors

A, B) Immunohistochemical labeling for NKA (green) in adult *Xenopus laevis* retina *B)* higher magnification of labeled photoreceptors shown adjacent to transmitted light image. Transgenic *X. laevis* tadpoles expressing *C)* GFP-NKA α3, *D)* GFP-NKA α1, or *E)* GFP-NKA α4 in rods. Nuclei labeled with Hoechst. Abbreviations: OS, outer segment; IS, inner segment; CP, calycal processes; ONL, outer nuclear layer; N, nuclei; OPL, outer plexiform layer; ST, synaptic terminal; INL, inner nuclear layer; IPL, inner plexiform layer; GC, ganglion cell layer.

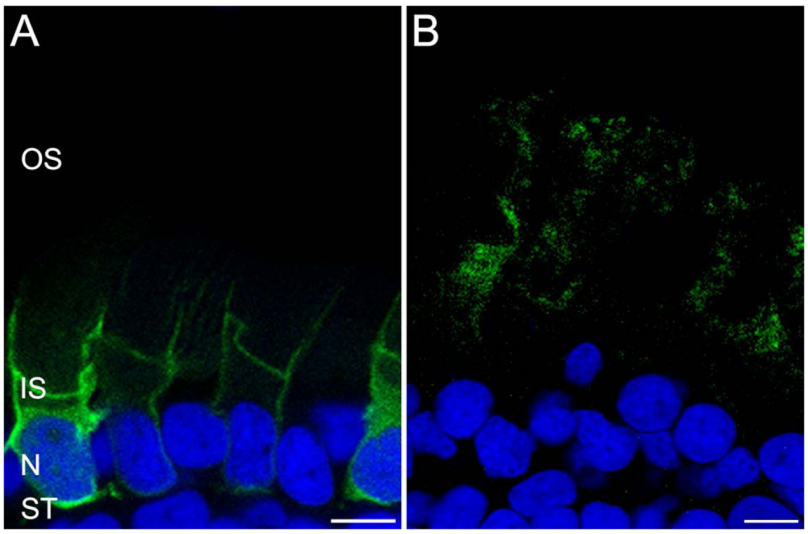

Figure 5. The N-terminus of NKA alpha subunits contains targeting information

A) A GFP-tagged chimera consisting of amino acids 1-82 from α3 and 89-1029 from α4 localizes to the ISPM. *B)* The complimentary chimera consisting amino acids 1-88 from α4 and 83-1025 from α3 localizes to OS. Nuclei labeled with Hoechst. Abbreviations: OS, outer segment; IS, inner segment; N, nuclei; ST, synaptic terminal. Scale bars are 5 μm.

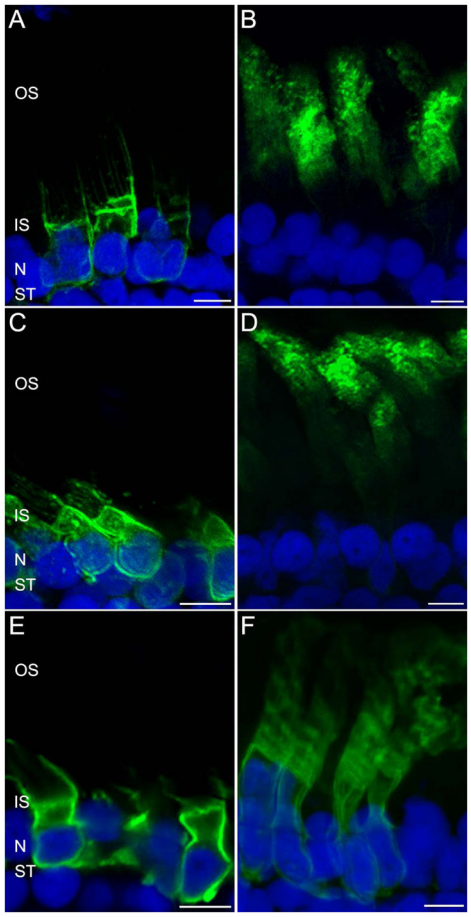

Figure 6. Targeting information is within the first 14 amino acids of NKA

GFP-tagged chimeras containing the N-terminus of NKA α3 localize to the ISPM, *A)* amino acids 1-38 from α3 and 45-1029 from α4, *C)* 1-24 from α3 and 23-1029 from α4, *E)* 1-14 from α3 and 13-1029 from α4. GFP-tagged chimeras containing the N-terminus of NKA α4 localize to the OS, *B)* amino acids 1-44 from α4 and 39-1025 from α3, *D)* 1-24 from α4 and 25-1025 from α3, *F)* 1-14 from α4 and 15-1025 from α3. Nuclei labeled with Hoechst, abbreviations and scale bars as in Figure 4.

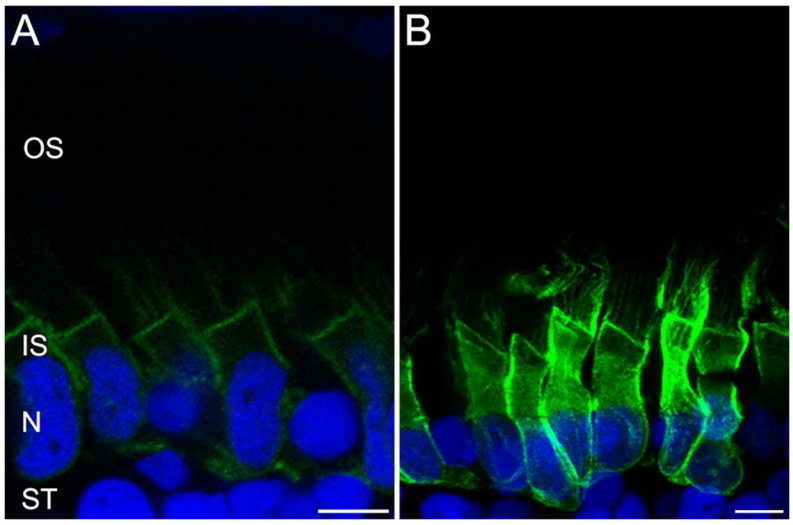

Figure 7. The first 14 amino acids of NKA α4 are required for outer segment localization

A) Deleting the first 14 amino acids from NKA α3 does not prevent ISPM localization. *B)* Deleting the first 14 amino acids from NKA α4 results in ISPM localization. Nuclei labeled with Hoechst, abbreviations and scale bars as in Figure 4.

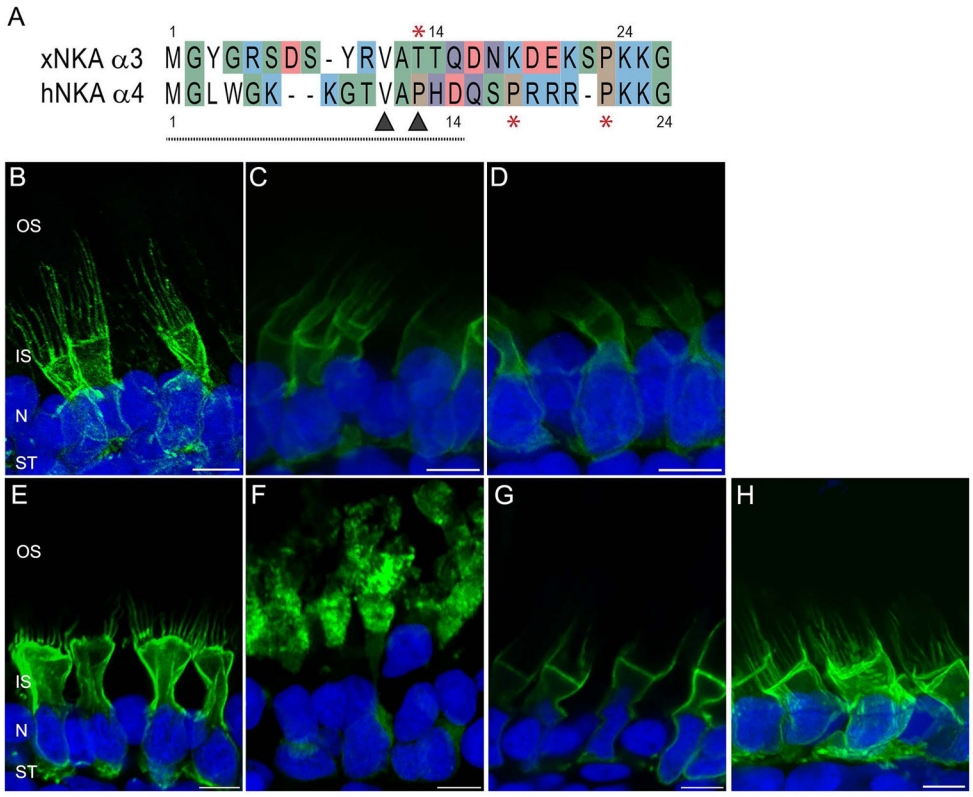

Figure 8. Identification of individual residues required for outer segment localization of NKA α4

A) Alignment of the N-terminal amino acids from *Xenopus* NKA α3 and human NKA α4; dashed line indicates sequence required for OS localization, triangles indicate a VxP motif, red asterisks indicate other residues mutated in the following panels. Color coding of amino acids: green, small polar; purple, polar; white, hydrophobic; blue, positively charged; red, negatively charged; brown, proline. *B)* Mutations, V10A and P12A results in ISPM localization of NKA α4. The individual mutations, V10A (*C*), or P12A (*D*) have the same affect. *E*) The T13P mutation in NKA α3 introducing a VxP motif was insufficient to change ISPM localization. *F)* Mutation of prolines 17 and 21 downstream of the VxP motif in NKA α4 did not prevent OS targeting. Deletions of amino acids *G)* 15-24, or *H)* 1-44 in NKA α3 did not prevent ISPM targeting. Nuclei labeled with Hoechst, abbreviations and scale bars as in Figure 4.

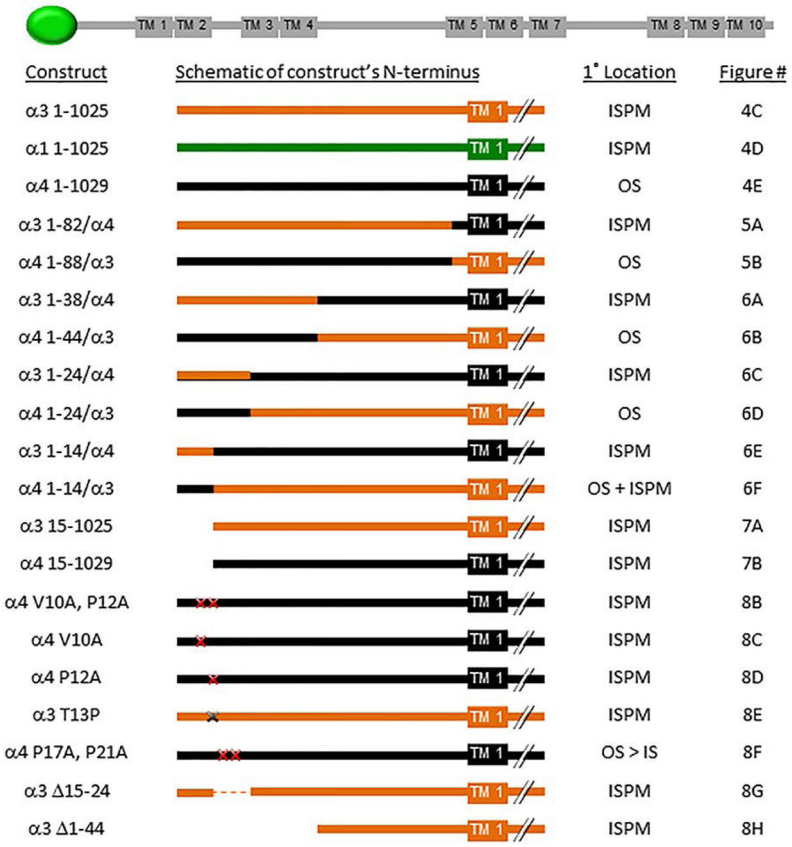

Figure 9. A summary of the design and targeting behavior of all constructs expressed in transgenic *Xenopus* photoreceptors

The linear arrangement of sequence motifs in NKA are shown on top. *Xenopus laevis* NKA α3 is shown in orange, human NKA α4 is shown in black, red asterisks indicate individual amino acid substitutions. Abbreviations: TMD, transmembrane domain; ISPM, inner segment plasma membrane; OS, outer segment.